CHIN. PHYS. LETT. Vol. 29, No. 7 (2012) 077308

Polarization-Selective Collimation Effect with a Reflective Plasmonic Cavity *

MAO Fei-Long(毛飞龙), XIE Jin-Jin(谢锦锦), FAN Qing-Yan(范庆言),
ZHANG Li-Jian(张立建), AN Zheng-Hua(安正华)**

Institute of Advanced Materials, State Key Laboratory of Surface Physics and Key Laboratory of Micro and Nano Photonic Structures (Ministry of Education), Fudan University, Shanghai 200433

(Received 27 April 2012)

We report that a metal-dielectric-metal cavity with a perforated top metallic film shows a remarkable polarization-selective collimation effect through reflection on the perforated film. According to simulations, such plasmonic cavities can achieve nearly perfect absorption (R<1.5%) of a transverse magnetic (TM) wave at an optimized incident angle while nearly perfect reflection (R∼100%) at normal incidence. A very wide incident angle range (approximately 15°–65°) is found to exhibit a high absorption ratio exceeding over 70%. In contrast, for a transverse electric (TE) wave, the plasmonic cavities remain highly reflective ($R \sim 100\%$) regardless of the incident angles. We elucidate that this polarization- and angle-dependent behavior arises from an even-order ($N = 2$) horizontal Fabry–Pérot (FP) resonant mode inside the plasmonic cavity. This effect may find potential applications for angle filtering of polarized divergent light beams in optics.

PACS: 73.20.Mf, 71.36.+c, 42.79.Dj DOI: 10.1088/0256-307X/29/7/077308

Recently, the metal-insulator-metal (MIM) cavity with a perforated top metallic slab has attracted tremendous interest because of its outstanding capability in subwavelength light confinement and its high coupling efficiency of far-field light into the near field.[1–4] This strong light confinement significantly increases light-matter interaction.[5] For example, by inserting semiconductor quantum wells into the cavity, strong coupling and even ultrastrong coupling between microcavity optical mode and quantum well intersubband transition were observed.[6–8] A variety of applications of this cavity have been explored, such as infrared photodetectors,[9] Fabry–Pérot interferometers,[10] and plasmonic thermal emitters.[11]

Here we study an MIM cavity whose top metallic slab is perforated with rectangular holes. In a certain frequency range, it is found that this plasmonic cavity greatly absorbs a transverse magnetic (TM) wave under oblique incidence but reflects almost 100% of the TM wave under normal incidence. For a transverse electric (TE) wave, however, the reflectivity stays at almost 100%, independent of the incident angles. Therefore, for a divergent TM wave with different incidence angles incident onto the cavity, the reflection beam will exhibit better directivity and parrellelism, which behaves like a collimation effect. For a TE wave, because the reflectivity remains almost at 100% regardless of incident angle, the reflection wave will keep the directional properties of the incident wave according to reflection law. Thus, this cavity shows a polarization-selective collimation effect through reflection. By numerical studies, we reveal that this interesting effect can be attributed to an even-order ($N = 2$) horizontal Fabry–Pérot (HFP) resonance inside the cavity.

Figure 1 schematically shows the structure of the proposed plasmonic cavity, in which the top metal layer is a Au film perforated with rectangle hole arrays and the bottom one is a continuous Au film. A dielectric spacer of Si with a fixed thickness of 1 μm is adopted to separate the two gold films. Each rectangular hole has a length L, width W, and the periodicities of the hole array are P_x in x-axis and P_y in y-axis. Since the rectangular hole is only sensitive to the light component with its electric field vector being perpendicular to the hole length,[12] in this work, the electric vectors are chosen to be always perpendicular to the hole length (L) for both the incident TM (or p-polarization) wave and the TE (or s-polarization) wave. As show in Fig. 1, the TM wave lies in the xz plane while the TE wave lies in the yz plane. Numerical simulation is performed by using the finite-difference time-domain (FDTD) method.[13] The dielectric constant of Au is assumed to follow a standard Drude model with parameters of $\varepsilon_\infty = 1$, $\omega_p = 1.365 \times 10^{16}$ rad/s, and $\gamma = 5.78 \times 10^{13}$ Hz, and the sandwiched Si layer is assumed to be a normal dielectric with $\varepsilon_{\rm Si} = 11.9$.

Figure 2 shows the reflection spectra of TM and TE waves with different incident angles. In case of normal incidence (0°), TE and TM excitations approach identical incident configurations and therefore show the same spectra. The first resonance appears at

*Supported by the National Basic Research Program of China Grant No 2009CB929300, the National Natural Science Foundation of China under Grant Nos 10804019, 11174055 and 11174057, Shanghai Science and Technology Committee (No 09dj1400103).

**Corresponding author. Email: anzhenghua@fudan.edu.cn

© 2012 Chinese Physical Society and IOP Publishing Ltd

about 17 THz and can be assigned to the fundamental localized shape resonance (LSR) of the rectangle holes.[14,15] The LSR mode is mainly determined by the hole shape and its geometrical sizes, and the resonant frequency ($f_{\rm LSR}$) can be estimated according to[16,17]

$$f_{\rm LSR} = \frac{c}{2L \cdot n_{\rm eff}}, \ n_{\rm eff} = \sqrt{\frac{\varepsilon_{\rm Si} + \varepsilon_{\rm air}}{2}}, \qquad (1)$$

where c is the light speed in vacuum and $n_{\rm eff}$ is the effective refraction index of the cavity structure for LSR mode, $\varepsilon_{\rm Si}$ and $\varepsilon_{\rm air}$ are dielectrics of silicon and air, respectively (the formula for $n_{\rm eff}$ in Eq. (1) applies to the case where the insulators on two sides of the metal layer are half-infinite. Here we use the same formula to roughly estimate $n_{\rm eff}$ value for our plasmonic cavity case). The other two resonances at higher frequencies (∼28 and ∼34 THz) are hybridized modes of propagating surface plasmons with different orders, whose origins are proved to be complex.[18] For oblique incidence, besides the LSR resonance, there appears to be an additional reflection dip at the frequency of 23–25 THz for TM excitation (Fig. 2(a)). The minimum reflectivity can be near to 0 for TM wave at 40°. However, for the TE wave, the reflectivity of 20° and 40° at this frequency remains almost unchanged from normal incidence.

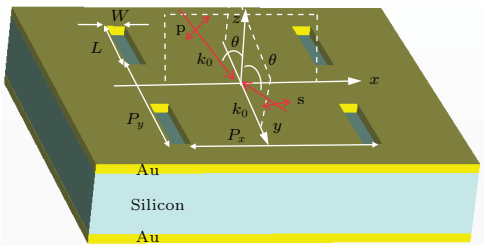

Fig. 1. Schematic diagram of a plasmonic cavity and the incident configuration for TE and TM waves. The top Au film is perforated with rectangular hole arrays, the bottom Au film is continuous, the sandwiched layer is silicon. Note that for both TM and TE polarizations, the electric field vectors are perpendicular to the hole length direction.

To further show the reflection spectra dependence on incident angle for TM and TE waves, we calculate the reflection spectra with the incident angle from 0–70°, the result is shown in Figs. 3(a) and 3(b). In 23–25 THz, for a very wide angle range, the cavity is able to absorb TM light well, e.g., over 70% maximum absorption can be achieved for 15–65°. In comparison, as shown in Fig. 3(b), the reflectivity of TE light remains nearly unity in the studied incident angle range (0–70°). From Fig. 3(a), we can see that normal incident and slightly oblique incident light have high reflectivity while middle or higher oblique incident light have low reflectivity. Therefore, when a 24 THz TM wave is incident onto the cavity with different incident angles, in the reflected beams, the proportion of normal or near normal light will increase and thus show a collimation-like effect. Hereafter, to ease our discussion, we term this resonance as collimation resonance (CR). From Fig. 3(a), with increasing incident angle, there is a slight redshift of the collimation resonance. As a result, the absorption shows different angle dependence for different frequencies. Figure 3(c) shows the reflection spectra of three selected frequencies from collimation resonance area, as can be seen, for each frequency, the maximum absorption (minimum reflection) locates at different angles. Therefore, in order to have an optimum collimation effect, one should consider the angle distribution of the incident light, because the reflection light will be the product of incident light and reflectivity-angle function. For instance, if the incident light angle is 0–25°, one should choose the 24.5 THz like reflectivity-angle function, then the right part of the function (high reflectivity for high oblique light) plays no effect. It is noteworthy mentioning that the CR effect can be applied in wider frequency ranges since the geometrical parameters of the cavity can be rescaled according to the scaling law.

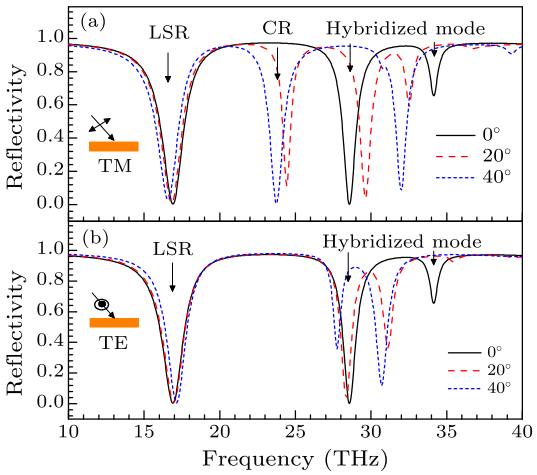

Fig. 2. The reflection spectra of TM and TE waves with different incident angles. The lateral geometric parameters are fixed at $P_x = P_y = 3.5\,\mu$m, $L = 3.3\,\mu$m, $W = 0.56\,\mu$m.

Table 1. Collimation resonance frequency calculated from the FDTD method and the $N = 2$ HFP mode frequency calculated from revisory Eq. (2).

Period P_x (μm)	FDTD (THz)	HFP (N=2)
3.2	27.2	27.2
3.4	25.6	25.6
3.6	24.3	24.2
3.8	23.1	22.9
4	22.0	21.8

To understand the physical origin of the CR resonance, we systematically studied its dependences on hole and array parameters. It turns out that the CR resonance is insensitive to the hole length L and array periodicity P_y, but changes dramatically with differ-

ent values of P_x and W. Figures 4(a) and 4(b) depict the reflection spectra for a TM wave with different periodicity P_x (Fig. 4(a)) and hole width W (Fig. 4(b)) at a fixed incident angle of 15°. As can be seen from Fig. 4, the collimation resonance redshifts with increasing P_x (Fig. 4(a)) while blueshifts with increasing W (Fig. 4(b)). The qualitative tendencies can be well reproduced by the horizontal Fabry–Pérot (HFP) modes along the x-axis inside the cavity, which was observed previously and also believed to be present in an MIM cavity structure with one-dimensional grating for the top metal layer.[4,5] The HFP frequency satisfies

$$f_{\mathrm{HFP}} = \frac{Nc}{2(P_x - W)n_{\mathrm{Si}}}, \tag{1}$$

where f_{HFP} is the frequency of the Nth order horizontal Fabry–Pérot mode, c is the speed of light in vacuum, P_x is the period of the hole array along the x-axis, W is the hole width, and n_{Si} is the refractive index of Si filling the cavity.

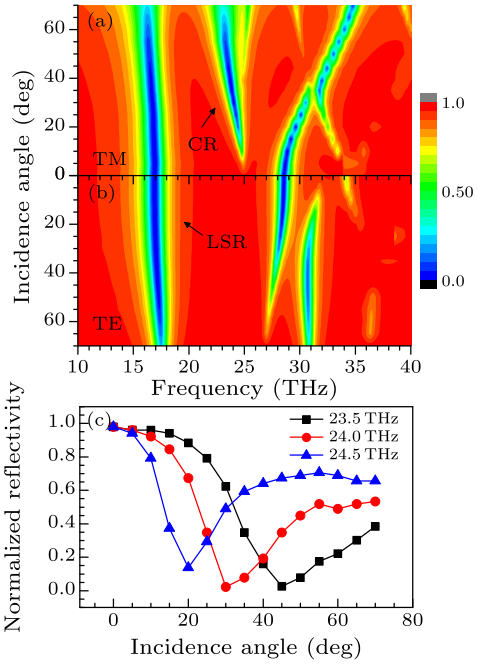

Fig. 3. Contour plots of reflection spectra of (a) TM and (b) TE polarizations with different incident angles, the lateral geometric parameters are fixed at $P_x = P_y = 3.5\,\mu\mathrm{m}$, $L = 3.3\,\mu\mathrm{m}$, $W = 0.56\,\mu\mathrm{m}$. (c) Reflectivity dependence on incidence angle for three selected frequencies (23.5, 24.0, and 24.5 THz).

In this work, the collimation resonance corresponds to f_{HFP} with $N = 2$. This Fabry–Pérot mode forms because of the impedence mismatch at the entrance and exit apertures, as schematically shown in Fig. 4(c). Ideally, the impedance mismatch takes place at boundaries between the air/Si/Au layer and the Au/Si/Au layer (vertical dashed lines in Fig. 4(c)).[5] When light is coupled into the cavity through a hole opening, part of the light will be reflected at the left boundary (vertical dashed line) and the other penetrating part will enter the Au/Si/Au tri-layer region. Due to reflections at both (left and right) boundaries, the trapped light can form a standing wave, that is, the HFP mode within a cavity length of $P_x - W$. Practically, in our plasmonic cavity (with two-dimensional array structures in the top Au film), because of the complex fringe field distributions of rectangular holes, the impedance-mismatching boundaries are not well defined by the vertical lines, as shown in Fig. 4(c), and the cavity length of the HFP mode can be slightly longer than $P_x - W$. Table 1 displays the simulated collimation resonance frequency and the analytical values of HFP ($N = 2$) calculated from revised Eq. (2) (to counteract the effect of a not-well-defined cavity length of the HFP mode, we replace $P_x - W$ with P_x in Eq. (2) for this analytical calculation). Excellent agreements are found between the simulated values and the analytical ones. This excellent agreement, as well as the strong angle-dependence of the depth of reflection dip (but very weak angle-dependence of resonant frequency), convince us that the CR indeed comes from the HFP eigenmode. Figure 4(c) shows the instantaneous fields of CR at a phase corresponding to the strongest enhancement. The electric vector clearly depicts second-order horizontal Fabry–Pérot mode properties with a two-node standing wave pattern and approximately one wavelength cavity length.

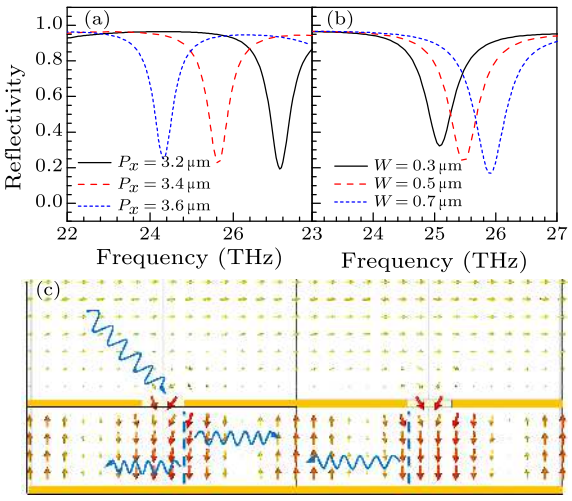

Fig. 4. Reflection spectra calculated using various typical hole array parameters for a TM wave at a fixed incident angle 15°. (a) $P_x = 3.2$, 3.4 and 3.6 μm, $P_y = 3.4\,\mu\mathrm{m}$, $L = 3\,\mu\mathrm{m}$, and $W = 0.56\,\mu\mathrm{m}$; (b) $W = 0.3$, 0.5, 0.7 μm, $P_x = P_y = 3.4\,\mu\mathrm{m}$, and $L = 3.2\,\mu\mathrm{m}$. (c) The electric field distribution of a collimation resonance at a phase corresponding to the strongest enhancement.

Finally, we mention why only the $N = 2$ horizontal Fabry–Pérot mode is observed in our system. This is because the $N = 1$ horizontal Fabry–Pérot mode (expected to appear at ∼12 THz from Eq. (2)) is well below the cutoff frequency of rectangular holes, as im-

plied by Eq. (1), where $n_{\rm eff} < n_{\rm Si}$. While for higher orders of horizontal Fabry–Pérot mode, a strong hybridization effect with other plasmonic resonances occurs (as implied by Figs. 3(a) and 3(b)). Therefore, it is not easy to well identify pure HPF modes. For the polarization dependence, as seen from Fig. 4(c), the E_z component is necessary for the excitation wave to overlap with the wavefunction of HFP mode in which E_z is dominant. Eventually only oblique incident TM (but not TE) waves can excite this HFP mode. As to the weak angle-dependence of the HFP resonant frequency, we surmise that it comes from the slight change of cavity length of the HFP mode with the increasing incident angles.

In summary, we report that a plasmonic cavity shows a polarization-selective collimation effect through reflection on the patterned metallic slab, it reflects a TM wave 100% under normal incidence (0°) while absorbs over 70% in a wide angle range from 15°–65°. However, this collimation effect is absent for TE polarization. We reveal that the $N = 2$ horizontal Fabry–Pérot mode is responsible for this interesting collimation effect. This polarization-selective collimation effect can find potential applications in angle-filtering of divergent light beams in optics.

References

[1] Hibbins A P and Sambles J R 2004 *Phys. Rev. Lett.* **92** 143904
[2] Miyazaki H T and Kurokawa Y 2006 *Phys. Rev. Lett.* **96** 097401
[3] Unlu M S and Strite S 1995 *J. Appl. Phys.* **78** 607
[4] Yodorov Y et al 2010 *Opt. Express* **18** 13886
[5] Yodorov Y et al 2009 *Phys. Rev. Lett.* **102** 186402
[6] Jouy P et al 2011 *Appl. Phys. Lett.* **98** 231114
[7] Yodorov Y et al 2010 *Phys. Rev. Lett.* **105** 196402
[8] Li M Z, An Z H, Zhou L, Mao, F L and Wang H L 2011 *Chin. Phys. Lett.* **28** 075206
[9] Hu X H, Li M, Ye Z, Leung W Y, Ho K M and Lin S Y 2008 *Appl. Phys. Lett.* **93** 241108
[10] Kang G G, Vartiainen I, Bai B F, Paakkonen P and Turunen J 2011 *Opt. Lett.* **36** 1011
[11] Ye Y H et al 2008 *Appl. Phys. Lett.* **93** 033113
[12] Jiang Y W, Tzuang L D, Ye Y H, Wu Y T, Tsai M W, Chen C Y and Lee S C 2009 *Opt. Express* **17** 2631
[13] CONCERTO 7.0 2008 Vector Fields Limited (England)
[14] Degiron A, Lezec H J, Yamamoto N and Ebbesen T W 2004 *Opt. Commun.* **239** 61
[15] Chen C Y, Tsai M W, Chuang T H, Chang Y T and Lee S C 2007 *Appl. Phys. Lett.* **91** 63108
[16] Wang H L et al 2011 *Plasmonics* **6** 319
[17] Mary A, Rodrigo S G, Martín-Moreno L and García-Vidal F J 2007 *Phys. Rev.* B **76** 195414
[18] Mao F L, An Z H, Xiao S Y, Komiyama S, Lu W and Zhou L 2012 *Small* (submitted)